Detection of Emerging through-Wall Cracks for Pipe Break Early Warning in Water Distribution Systems Using Permanent Acoustic Monitoring and Acoustic Wave Analysis

Jinzhe Gong [1,2] · Martin F. Lambert [1] · Mark L. Stephens [3] · Benjamin S. Cazzolato [4] · Chi Zhang [1,3]

Abstract

Smart water networks, created using Internet of Things (IoT) technologies, have been increasingly adopted by water utilities across the world. This research focuses on the use of smart water technologies for detecting newly formed through-wall pipe cracks and leaks in water distribution systems for the purpose of pipe break early warning and prevention. This research develops easy-to-implement algorithms for analysing the hydro-acoustic vibration wave files regularly collected by permanently installed accelerometers in a water network, and for generating alarms when small leaks from developing pipe cracks are detected. Descriptive features of the historical wave files are investigated for five sites where newly-formed pipe cracks were detected nearby. It is found that the median frequency (MF) and the root-mean-square (RMS) values derived from the wave files are useful indicators for detecting new cracks and leaks. The confidence of pipe crack detection in noisy city environments can be significantly increased by windowing each already short-duration wave file into a number of frames with even shorter durations, and analysing the behaviour of the MF and RMS values of all the frames to look for the persistence of the leak feature even when part of the signal is contaminated with interference. The results show that the developed technique can robustly detect new through-wall cracks and leaks in a timely manner, and is tolerant of interference from customer water use and transient environmental noise.

Keywords Accelerometer · Leak detection · Leak-before-break · Pipe break · Smart water network

✉ Jinzhe Gong
james.gong@deakin.edu.au

Extended author information available on the last page of the article

1 Introduction

The concept of Smart Water Network (SWN) is relatively new, but it has been recognised as a tremendous opportunity for water authorities to achieve significant financial savings and address global issues such as water safety and quality (Walsby 2013). Research and development related to SWN has intensified in the past decade, covering diverse topics such as leak detection and management (Stoianov et al. 2007; Gupta and Kulat 2018), pipe break detection (Allen et al. 2012), smart metering (Savić et al. 2014), sewer overflow monitoring and prevention (Boulos 2017) and wireless sensor networks (Obeid et al. 2016).

With regard to leak detection in water distribution systems (WDSs), acoustic techniques using portable acoustic correlators and listening devices (e.g. ground microphones and listening sticks) are the most commonly used (Gupta and Kulat 2018). Because the implementation is labour intensive, they are typically used only when leaks are suspected in a specific pipe or in a small area. Recent development of wireless acoustic and pressure sensors have enabled long-term/permanent installation and regular/continuous monitoring for leak and pipe break detection in water pipelines (Obeid et al. 2016). The sudden failure of a pipe will introduce short-lived transient pressure waves with specific characteristics that propagate along the pipe, which can be measured by multiple transient pressure sensors for event detection and triangulation of the source (Srirangarajan et al. 2013). However, small pipe breaks (<5 L/s discharge) are difficult to detect because the critical information embedded in the break-induced transient wave can be significantly compromised by wave dissipation and dispersion (Gong et al. 2018). In addition, pipe break detection is still a reactive practice, since it only reports the incident after its occurrence.

Regular/continuous monitoring by distributed acoustic sensors, such as accelerometers or hydrophones, is considered to be more suitable for the detection of smaller leaks for SWNs. Stoianov et al. (2007) developed one of the earliest prototype wireless acoustic sensor networks for pipeline leak detection. The principle is that a new leak manifests itself as additional energy in certain frequency bands in the spectrum of the acoustic measurement (Hunaidi and Chu 1999). In recent years, a number of acoustic-based leak detection techniques have been proposed using more advanced cross-correlation analysis (Gao et al. 2018) and feature extraction and pattern recognition algorithms (Jin et al. 2014). However, large scale applications to WDSs in noisy city environments are limited.

The research reported in the current paper focuses on the detection of newly emerged through-wall pipe cracks in the Adelaide city water network. The objective of this application is to prevent pipe breaks (and associated consequences) in busy city areas, which is different from conventional leak management in WDSs that is typically aimed at non-revenue water reduction. The authors have observed, for the Adelaide central-business-district (CBD) water network, that more than 50% of pipe breaks in ageing cast iron (CI) water pipes are preceded by steadily developing cracks and leaks (Stephens et al. 2018). This is also supported by other recent numerical and laboratory research, which adapted the leak-before-break (LBB) concept originated in the nuclear power industry (Bourga et al. 2015) to ageing CI water pipes (Rathnayaka et al. 2017). The current research is one of the pioneering studies on using the LBB for proactive pipe break control in WDSs.

The research develops an easy-to-implement technique for just-in-time pipe crack detection using permanently installed accelerometers. The research is field oriented and validated using the daily acoustic wave files collected by the Adelaide CBD SWN. Descriptive features of the historical wave files are investigated for five sites where newly developed through-wall pipe

cracks have been confirmed nearby. It is found that the median frequency (MF) and the root mean square (RMS) are useful indicators for detecting new or developing cracks and leaks. The developed technique is tolerant to interference from customer water use and transient environmental noise.

2 The Acoustic Monitoring System in Adelaide CBD

The South Australian Water Corporation (SA Water) invested more than AUD $4 m on smart water technologies and established Australia's first comprehensive SWN in the Adelaide CBD in 2017 (Edmonds et al. 2018). Part of the SWN is an acoustic pipe crack monitoring system with 305 accelerometer sensors (Von Roll, Switzerland). The accelerometers are powered by two standard AA batteries, and installed in existing fire hydrant chambers, with the sensor head magnetically attached to the pipe fitting. The sensors are configured to measure a non-dimensional noise level every 10 min from 4 am to 2 am the next day, and every 5 min between 2 am and 4 am. At about 2:05 am each morning, a wave file is recorded with a sampling rate of 4681 Hz and a duration of 9.995 s. The sensors have an in-built high-pass filter with a cut-off frequency set at 10 Hz in this study and an in-built anti-aliasing filter. All the data is normally transferred to a cloud based storage once a day between 6 am to 7 am through the 3G mobile network. More details of the sensor network can be found in Stephens et al. (2018).

3 The Proposed Leak-Before-Break Detection Technique

The research focuses on the use of descriptive features derived from the measured wave files for the detection of new leaks induced by emerging through-wall pipe cracks. Descriptive features, such as the mean, the peak, the variance, the root-mean-square (RMS) and the median frequency (MF) values, etc., are easy to extract and analysis; therefore the analysis has the potential to be implemented cost-effectively.

The proposed detection algorithm is summarised in the flow chart shown in Fig. 1. The original acoustic wave files have been normalised to have a possible minimum value of −1 and a possible maximum value of 1. L90 means the threshold exceeded by 90% of the values in a data set. Detailed explanations are given in the following sections.

3.1 Key Indicators

The RMS and the normalised MF values are selected as key indicators for the detection of new through-wall pipe cracks and leaks. The RMS value of a vector $\{x_n\}$ ($n = 1 \ldots N$) is defined as

$$x_{RMS} = \sqrt{\frac{1}{N} \sum_{n=1}^{N} |x_n|^2} \tag{1}$$

where x_{RMS} is the RMS value, N is the total number of data in the vector. For the normalised acoustic wave files measured at the same location and on consecutive days, the feature of the RMS values over time also represents the trend of the standard derivation, the variance, and the energy. The appearance or the further development of a through-wall crack theoretically adds
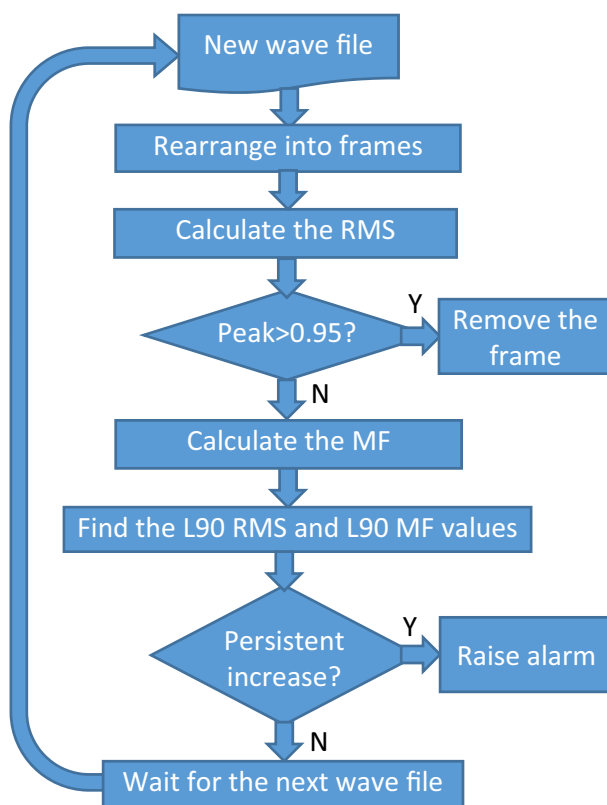
Fig. 1 Flowchart illustrating the steps of the proposed detection algorithm

additional energy to the measured acoustic signal and therefore increasing the amplitude of the acoustic vibration in the time domain and being reflected as an increased RMS value. Early studies have shown that, in general, a higher discharge flow tends to induce a higher RMS value (Jin et al. 2014; Butterfield et al. 2017). For the normalised acoustic wave files, the RMS value is always in the range of 0 to 1.

The MF value targets the feature of the leak-induced signals in the frequency domain. The MF value is the frequency at which the power spectrum is divided into two regions with equal energy. Background acoustic signals in WDSs are typically low in frequency, while the appearance of a new leak adds one or multiple high-frequency bands into the spectrum (Hunaidi and Chu 1999; Stoianov et al. 2007), which shifts the MF value to a higher frequency. In this research, the MF values are normalised by the Nyquist frequency (half of the sampling frequency) such that the value is always in the range of 0 to 1.

3.2 Practical Challenges and Counter-Measures

A key challenge in field application is the acoustic/vibration interference from non-leak sources. Common sources of interference in WDSs are traffic noise and noise from customer water use. The research has found that (as further illustrated in the section *Discussion*): the traffic noise is typically high in amplitude and can increase RMS values significantly, but the noise is a transient signal and generally in a frequency range lower than that of leak signals; the

customer water use has a signature very similar to leaks in the frequency domain, but the water use signal is typically accompanied by regular water meter ticking noise that is low in frequency.

This research has developed a technique to mitigate the challenges and reduce the false-alarm rates. Each measured acoustic wave file (~10 s in duration, 46,786 samples) is rearranged into a number of frames with a data length of 256 (duration of each frame ~55 ms). This is achieved by using a sliding rectangular window of 256 in length and with 80% overlap between windows. The frames that have a peak value close to the upper limit of unity are most likely to have been heavily contaminated by environmental noise and are removed before any further analysis (the threshold selected was 0.95 in this study). The RMS values for all the remaining frames are calculated. Due to the transient nature of the environmental noise, some frames are less contaminated than others and have lower RMS values, which better reflect the persistent acoustic energy on site.

The normalised MF values for all the remaining frames are determined. A new through-wall crack will introduce a leak and elevate the MF values consistently. For measurements that are predominately water use signals, a large number of frames will include the low-frequency water meter ticking noise, which can counteract the high-frequency leak sound, and therefore maintain relatively low MF values.

The RMS value(s) and the normalised MF value(s) at the lower bound are of interest based on the analysis above. To allow for variations, for each measured wave file, the RMS values and the normalised MF values are ranked from low to high, and the L90 values of the RMS and ML are selected as the indicators. They are noted as the L90 RMS value and the L90 MF value following the convention in acoustic monitoring and it means 90% of the values are higher than the indicator in each category.

The L90 RMS and L90 MF values are then calculated for all the wave files collected over time at specific measurement sites. The results are then plotted and updated when new data is available. A persistent increase in the L90 RMS and L90 MF values indicates the occurrence of a new through-wall crack in a pipe within the acoustic range of an accelerometer. Validation using field data (details in the following section) shows that the L90 MF is more robust than the L90 RMS value. It is suggested that the L90 MF value be used as the main indicator for leak detection.

4 Field Validation

The proposed detection technique is validated using the historical wave files collected at five sites where newly-formed longitudinal and circumferential pipe cracks have been confirmed nearby. The acoustic sensors involved are labelled POS14, POS111, POS192, POS244 and POS268. The results are given in Figs. 2, 3, 4, 5 and 6 and summarised in Table 1.

4.1 Sensor POS14

Figure 2 shows that, at POS14, the new leak from a circumferential crack on a CI water main can be successfully detected by the change in L90 MF values. This was the first cracked pipe detected by the Adelaide SWN and more information, including a photo of the crack, is reported in Stephens et al. (2018). The L90 MF rose from a normalised value of about 0.05 on and before 22 July 2017 to more than 0.7 on 23 July 2017. The high L90 MF values persisted

Fig. 2 L90 RMS and L90 MF
values calculated for acoustic
sensor POS14
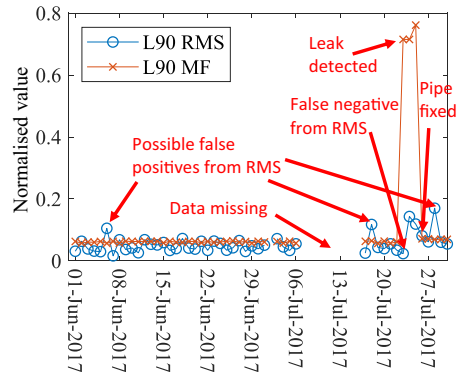
until the cracked pipe was fixed. On the no-leak days prior to and after the leak event, the L90
MF values remained low.

The L90 RMS value at POS14, however, was still low on the first day of the leak (23
July 2017), which is a false negative if considered in isolation. It increased on the following
days as the crack further developed, reinforcing the alarm raised by the L90 MF values. On the
other hand, the L90 RMS values were relatively high on some no-leak days (6 June 2017, 18
July 2017 and 28 July 2017), which can contribute to possible false positives if considered in
isolation. Further investigation into the wave files confirm that the false positives from the L90
RMS values on 6 June 2017 and 28 June 2017 were induced by traffic noise, and the one on 18
July 2017 was induced by noise from rainfall.

4.2 Sensor POS111

At sensor POS111, both the L90 MF values and the L90 RMS values responded to the leak
from a circumferential crack on a CI water main which started on 12 December 2017. Higher
values persisted until 11 January 2018, after which the cracked pipe was fixed. An interesting
finding is that, before the event, both the L90 MF values and L90 RMS values were relatively
low and stable; however, after the repair work, while the L90 RMS values went back to the
original low level, the L90 MF values shifted between low and high on different days,
generating irregular false positives. Examination of the post-repair wave files and maintenance
history revealed that the unstable L90 MF values were induced by poor physical contact
between the accelerometer sensor head and the fire hydrant fitting in the chamber. It is

Fig. 3 L90 RMS and L90 MF
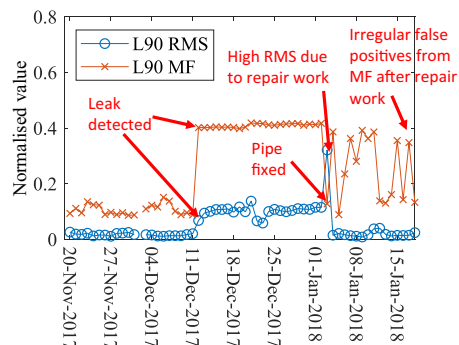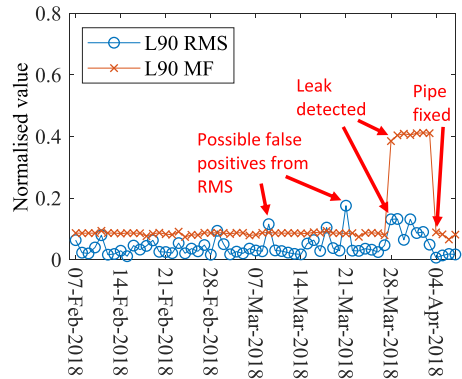values calculated for acoustic
sensor POS111

Fig. 4 L90 RMS and L90 MF values calculated for acoustic sensor POS192

believed that the sensor was removed and reattached during the repair work. As a result, an unstable L90 MF trace can be used as an indicator for, among other things, sensor malfunctions.

4.3 Sensor POS192

At sensor POS192, the L90 MF was low (normalised value <0.1) and stable before and after the leak event, and was high (normalised value >0.4) during the event (a circumferential crack on a CI water main). The L90 RMS values were relatively higher during the event but unstable. On some days (e.g., 9 March 2018 and 21 March 2018), the L90 RMS values were high and could result in false positives if considered in isolation. Further examination of the wave files confirmed that the L90 RMS false positives were induced by transient noise, including traffic noise.

4.4 Sensor POS244

Sensor POS244 was moved into place on 8 February 2018 to monitor a known leak nearby (a short longitudinal crack on a CI water main). It was installed after the scheduled wave recording time of 2:05 am such that the leak signal was not captured on the day, but high L90 MF values and L90 RMS values were observed from 9 February 2018. The leak and cracked pipe were fixed by 14 February 2018 and the L90 MF values and the L90 RMS values

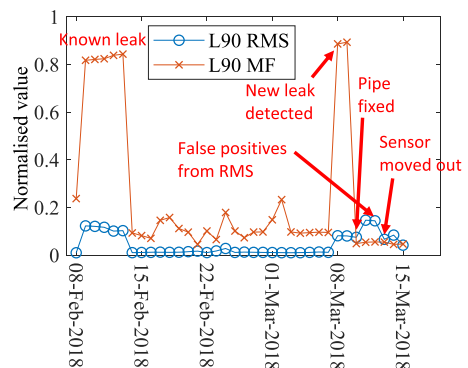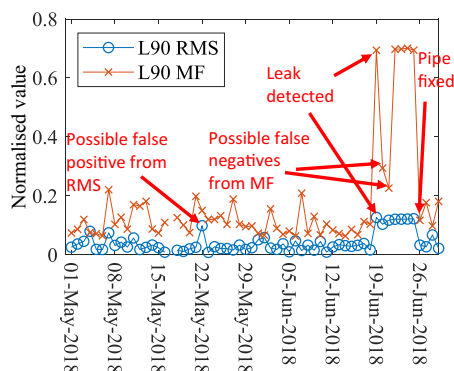Fig. 5 L90 RMS and L90 MF values calculated for acoustic sensor POS244

Fig. 6 L90 RMS and L90 MF
values calculated for acoustic
sensor POS268

dropped thereafter as expected. A new leak (a circumferential crack, at a different location from the first longitudinal crack) occurred later and was reported by elevated L90 MF and L90 RMS values from 8 March 2018. The L90 MF values dropped to a lower level on 10 May 2018 after the leak was fixed.

4.5 Sensor POS268

Both the L90 RMS and the L90 MF values elevated following a new leak event (a circumferential crack on a CI water main) on 19 June 2018. The L90 RMS values remained high until 25 June 2018 when the cracked pipe was fixed. The L90 MF values dropped to a relatively lower level on 20 and 21 June 2018, which could contribute to false negatives if considered in isolation. Further examination of the wave files confirmed that the lower L90 MF value on 20 June 2018 was caused by low-frequency traffic noise. The lower L90 MF value on 21 June 2018 was caused by low-frequency water meter noise. The L90 RMS value was relatively high on 22 May 2018 and it could contribute to a false positive if considered in isolation. This higher L90 RMS value was caused by water use and meter noise that persisted over the duration of the wave file.

4.6 Summary of Results

The average RMS and MF values before the leak event (background) and during the leak event for the five cases have been summarised in Table 1, together with the distance from the sensor to leak, the street where the cracked pipe is located, pipe age and pipe nominal diameter. All the five pipes involved are cast iron cement lined (CICL) pipes.

Table 1 Summary of results for the case studies

Sensor	Background Average RMS&MF	Leak Average RMS&MF	Distance (m)	Pipe location	Pipe age (Yr)	Nom. Diam. (mm)
POS14	0.05&0.06	0.09&0.73	15	Liverpool St	88	100
POS111	0.02&0.11	0.10&0.41	7	Flinders St	49	150
POS192	0.04&0.09	0.10&0.41	42	St Johns St	53	150
POS244	0.01&0.11	0.08&0.89	15	Gilles Ln	51	100
POS268	0.03&0.11	0.12&0.57	36	Cannon St	42	150

It can be seen from Table 1 that the background RMS and MF are generally smaller than 0.05 and 0.11, respectively, while the leak induced RMS and MF are generally greater than 0.08 and 0.41, respectively. The difference serves as the foundation for differentiating leak-induced signals from background noise. However, both the background and leak-induced RMS and MF values vary in relative wide ranges across the five cases, and there is no simple correlation to the location of the leak or to the pipe age and diameter. For example, for POS111 on Flinders Street, the leak was only 7 m to the sensor, but the average leak-induced RMS and MF values are almost the same (after rounding) to the case at POS192 on St Johns Street, where the leak was 42 m away. Note that both pipes have a nominal diameter of 150 mm and at a similar age. One complexity is that the recorded wave signal is also dependent on the contact condition between the sensor head and the pipe fitting. More research is needed to investigate whether general relationships can be established to link specific RMS and MF values to the leak and pipe properties.

5 Discussion

5.1 Impact of Traffic Noise

Traffic noise has been identified as the most common source of interference in the wave files for the Adelaide CBD. Figure 7 provides an example based on the wave file recorded by sensor POS14 on 6 June 2017. The spectrogram was calculated using the short-term Fourier transform (window length = 256, 80% overlapping). The running RMS and MF values were calculated using the same sliding window. It can be seen that the amplitude of the wave file gradually increased to the upper and lower limits and then gradually decreased. The spectrogram shows the energy of the low-frequency components increased and then decreased accordingly. This is associated with a vehicle moving towards and then away from the sensor station. The RMS values significantly increased during the time of 6 to 7.5 s, but were also affected at other times. In contrast, the MF values were generally stable and not significantly influenced by the traffic noise.

The pre-processing based on the peak value (Fig. 1) will remove frames with a peak value greater than 0.95 and therefore it can remove some of the data heavily contaminated by the traffic noise. In most cases, this pre-processing and the use of L90 RMS values have prevented false positives in the RMS indicator for data contaminated by traffic noise. However, because each wave file is short (a total duration of ~10 s), strong and extended traffic noise can still affect a significant portion of the data even after the pre-processing. This is the case for POS14 on 6 June 2017, which resulted in the relatively high L90 RMS values as seen in Fig. 2.

Most energy from the traffic noise is in the low-frequency range such that it is unlikely to induce false positives in the MF indicator [as confirmed in Fig. 7c]. However, it may introduce false negatives when strong traffic noise contaminates a leak-induced wave. Figure 8 provides an example, in which the wave file recorded by sensor POS268 on 20 June 2018 is shown, together with its spectrogram and the running RMS and MF values. The L90 MF value was relatively low for this day (Fig. 6) because more than 10% of the remaining frames were still contaminated by the noise even after the pre-processing. Increasing the wave file measurement duration and measurement frequency will mitigate the impact of transient environmental noise.

Fig. 7 Example of a wave file under the no-leak condition but contaminated by traffic noise: **a** the wave file, **b** its spectrogram, and **c** the running RMS and MF values; based on the recording by sensor POS14 on 6 June 2017
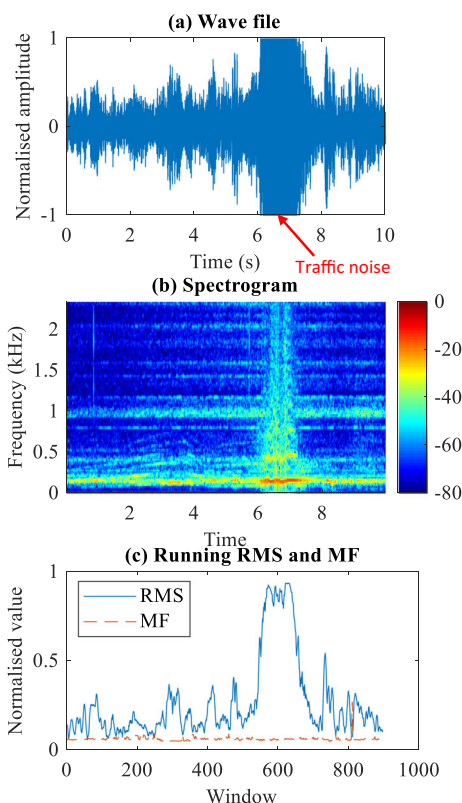
5.2 Impact of Water Usage and Water Meter

Water consumption from a branch or an off-take on the water main is similar to a through-wall discharge and generates similar acoustic waves, adding new and typically high-frequency bands to the spectrum. Different from real leaks on the water main, water consumption is typically accompanied by water meter ticking noise, which is regular and mainly low in frequency.

The measurements at POS268 were frequently contaminated by water use and water meter noise. Figure 9 illustrates an example, in which the wave file recorded by sensor POS268 on 13 May 2018 is shown, together with its spectrogram and the running RMS and MF values. The water meter sound had a regular interval as shown in Fig. 9a. A high-frequency band and a low-frequency band were observed in the spectrogram in Fig. 9b, which were from the water use and the meter ticking signals, respectively. The water meter ticking sound increased the RMS value while decreasing the MF value as shown in Fig. 9c.

Note that no false positive or false negative was generated on 13 May 2018 at POS268 as in Fig. 6. The low-frequency meter ticking sound balanced the high-frequency water use sound, which resulted in a low L90 MF value. The meter ticking sound was regular but not persistent (see Fig. 9) and therefore the L90 RMS value reflects the energy of the water use sound (which was not strong in this case). However, on 22 May 2018 at POS268, the L90 RMS value was relatively high due to stronger water use sound.

Fig. 8 Example of a wave file under the leaky condition but contaminated by traffic noise: **a** the wave file, **b** its spectrogram, and **c** the running RMS and MF values; based on the recording by sensor POS268 on 20 June 2018
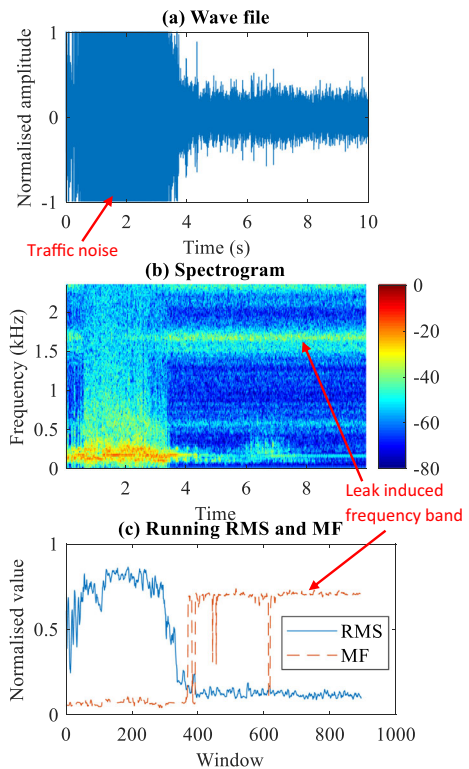

The water use and meter ticking signal, when mixed with the leak signal, can introduce false negatives for the MF indicator. This is because the low-frequency meter ticking sound can balance the high-frequency water use sound as well as the high-frequency leak sound, and results in a low L90 MF value. The result on 22 June 2018 at POS268 as shown in Fig. 6 is an example. More frequent data recording will reduce the likelihood of getting false negatives.

6 Conclusions

An easy-to-implement technique for the detection of emerging pipe leaks and cracks using permanently installed accelerometers has been developed. Short-duration wave files from the accelerometer are rearranged into a number of frames using a sliding window (~55 ms, 256 samples) with overlapping (80% in this study). A peak-value-based pre-processing technique has been proposed, which removes frames heavily contaminated by transient environmental noise. The detection is conducted by analysing the L90 MF and the L90 RMS values for all the remaining frames. A persistent increase in the L90 RMS and L90 MF values indicates the occurrence of a new leak in any pipe(s) monitored by an acoustic sensor. The technique has been validated using the daily acoustic wave files collected from five sites in the Adelaide CBD SWN. All developing cracks in the pipes would have been detected using the proposed technique.

A persistently elevated L90 MF value has been found to be a robust indicator for detecting new leaks and cracks. The L90 MF indicator is tolerant to traffic noise, which typically does

Fig. 9 Example of a wave file under the no-leak condition but contaminated by water consumption and water meter noise: **a** the wave file, **b** its spectrogram, and **c** the running RMS and MF values; based on the recording by sensor POS268 on 13 May 2018
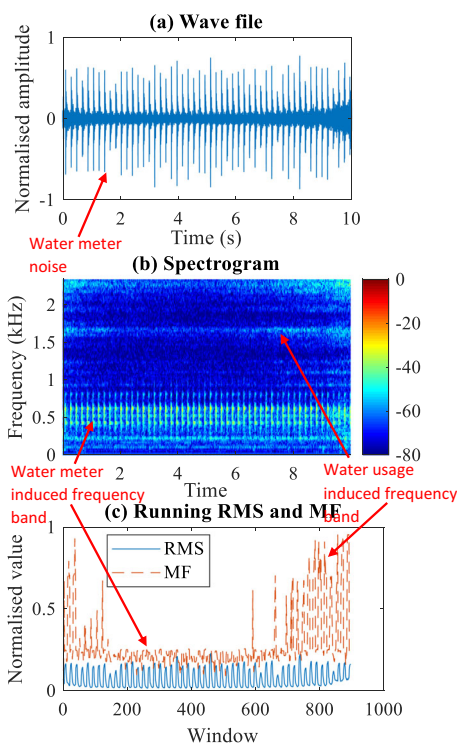
not last long and is skewed to the low-frequency range (compared to leak noise). Water meter noise associated with customer water use can reduce the L90 MF value even when real leaks are present. A persistently elevated L90 RMS value can be used to reinforce leak and through-wall crack detection. The L90 RMS value is not as robust an indicator as the L90 MF value when traffic noise, water use and water meter ticking noise are present.

The interference from traffic, water use and water meter ticking is unlikely to appear consecutively in multiple wave recordings, while a leak should generate persistent signals and therefore induce persistently elevated L90 MF and L90 RMS values. More frequent and longer wave file sound recordings will enhance the robustness of the detection.

Compliance with Ethical Standards

Conflict of Interest None.

References

Allen M, Preis A, Iqbal M, Whittle AJ (2012) Case study: a smart water grid in Singapore. Water Pract Technol 7(4). https://doi.org/10.2166/wpt.2012.089

Boulos PF (2017) Smart water network modeling for sustainable and resilient infrastructure. Water Resour Manag 31(10):3177–3188. https://doi.org/10.1007/s11269-017-1699-1

Bourga R, Moore P, Janin YJ, Wang B, Sharples J (2015) Leak-before-break: global perspectives and procedures. Int J Press Vessel Pip 129-130:43–49. https://doi.org/10.1016/j.ijpvp.2015.02.004

Butterfield JD, Krynkin A, Collins RP, Beck SBM (2017) Experimental investigation into vibro-acoustic emission signal processing techniques to quantify leak flow rate in plastic water distribution pipes. Appl Acoust 119:146–155. https://doi.org/10.1016/j.apacoust.2017.01.002

Edmonds H, Kuster E, Stephens M (2018) Adelaide CBD smart water network. In: Proceedings of the Ozwater'18 conference. Australian Water Association, Brisbane

Gao Y, Liu Y, Ma Y, Cheng X, Yang J (2018) Application of the differentiation process into the correlation-based leak detection in urban pipeline networks. Mech Syst Signal Process 112:251–264. https://doi.org/10.1016/j.ymssp.2018.04.036

Gong J, Nguyen STN, Stephens ML, Lambert MF, Marchi A, Simpson AR, Zecchin AC (2018) Correlation of post-burst hydraulic transient noise for pipe burst/leak localisation in water distributions systems. In: Proceedings of the 13th international conference on pressure surges. Cranfield, BHR Group

Gupta A, Kulat KD (2018) A selective literature review on leak management techniques for water distribution system. Water Resour Manag 32(10):3247–3269. https://doi.org/10.1007/s11269-018-1985-6

Hunaidi O, Chu WT (1999) Acoustical characteristics of leak signals in plastic water distribution pipes. Appl Acoust 58(3):235–254. https://doi.org/10.1016/S0003-682X(99)00013-4

Jin H, Zhang L, Liang W, Ding Q (2014) Integrated leakage detection and localization model for gas pipelines based on the acoustic wave method. J Loss Prev Process Ind 27:74–88. https://doi.org/10.1016/j.jlp.2013.11.006

Obeid AM, Karray F, Jmal MW, Abid M, Qasim SM, BenSaleh MS (2016) Towards realisation of wireless sensor network-based water pipeline monitoring systems: a comprehensive review of techniques and platforms. IET Sci Meas Technol 10(5):420–426. https://doi.org/10.1049/iet-smt.2015.0255

Rathnayaka S, Shannon B, Zhang C, Kodikara J (2017) Introduction of the leak-before-break (LBB) concept for cast iron water pipes on the basis of laboratory experiments. Urban Water J 14(8):820–828. https://doi.org/10.1080/1573062X.2016.1274768

Savić D, Vamvakeridou-Lyroudia L, Kapelan Z (2014) Smart meters, smart water, smart societies: the iWIDGET project. Procedia Eng 89:1105–1112. https://doi.org/10.1016/j.proeng.2014.11.231

Srirangarajan S, Allen M, Preis A, Iqbal M, Lim HB, Whittle AJ (2013) Wavelet-based burst event detection and localization in water distribution systems. J Signal Process Syst 72(1):1–16. https://doi.org/10.1007/s11265-012-0690-6

Stephens M, Gong J, Marchi A, Dix L, Wilson A, Lambert M (2018) Leak detection in the Adelaide CBD water network using permanent acoustic monitoring. In: Proceedings of the Ozwater'18 conference. Australian Water Association, Brisbane

Stoianov I, Nachman L, Madden S, Tokmouline T (2007) PIPENET: a wireless sensor network for pipeline monitoring. In: Proceedings of the 6th international symposium on information processing in sensor networks. IEEE, New York, pp 264–273. https://doi.org/10.1109/IPSN.2007.4379686

Walsby C (2013) The power of smart water networks. J Am Water Works Assoc 105(3):72–77. https://doi.org/10.5942/jawwa.2013.105.0038

Affiliations

Jinzhe Gong [1,2] · **Martin F. Lambert** [1] · **Mark L. Stephens** [3] · **Benjamin S. Cazzolato** [4] · **Chi Zhang** [1,3]

Martin F. Lambert
martin.lambert@adelaide.edu.au

Mark L. Stephens
mark.stephens@sawater.com.au

Benjamin S. Cazzolato
benjamin.cazzolato@adelaide.edu.au

Chi Zhang
raymond.zhang@sawater.com.au

[1] School of Civil, Environmental and Mining Engineering, University of Adelaide, North Terrace, Adelaide, SA 5005, Australia

[2] School of Engineering, Deakin University, 75 Pigdons Road, Waurn Ponds, VIC 3216, Australia

[3] Strategic Asset Management Department, SA Water, 250 Victoria Square, Adelaide, SA 5000, Australia

[4] School of Mechanical Engineering, University of Adelaide, North Terrace, Adelaide, SA 5005, Australia

Terms and Conditions

Springer Nature journal content, brought to you courtesy of Springer Nature Customer Service Center GmbH ("Springer Nature").

Springer Nature supports a reasonable amount of sharing of research papers by authors, subscribers and authorised users ("Users"), for small-scale personal, non-commercial use provided that all copyright, trade and service marks and other proprietary notices are maintained. By accessing, sharing, receiving or otherwise using the Springer Nature journal content you agree to these terms of use ("Terms"). For these purposes, Springer Nature considers academic use (by researchers and students) to be non-commercial.

These Terms are supplementary and will apply in addition to any applicable website terms and conditions, a relevant site licence or a personal subscription. These Terms will prevail over any conflict or ambiguity with regards to the relevant terms, a site licence or a personal subscription (to the extent of the conflict or ambiguity only). For Creative Commons-licensed articles, the terms of the Creative Commons license used will apply.

We collect and use personal data to provide access to the Springer Nature journal content. We may also use these personal data internally within ResearchGate and Springer Nature and as agreed share it, in an anonymised way, for purposes of tracking, analysis and reporting. We will not otherwise disclose your personal data outside the ResearchGate or the Springer Nature group of companies unless we have your permission as detailed in the Privacy Policy.

While Users may use the Springer Nature journal content for small scale, personal non-commercial use, it is important to note that Users may not:

1. use such content for the purpose of providing other users with access on a regular or large scale basis or as a means to circumvent access control;

2. use such content where to do so would be considered a criminal or statutory offence in any jurisdiction, or gives rise to civil liability, or is otherwise unlawful;

3. falsely or misleadingly imply or suggest endorsement, approval , sponsorship, or association unless explicitly agreed to by Springer Nature in writing;

4. use bots or other automated methods to access the content or redirect messages

5. override any security feature or exclusionary protocol; or

6. share the content in order to create substitute for Springer Nature products or services or a systematic database of Springer Nature journal content.

In line with the restriction against commercial use, Springer Nature does not permit the creation of a product or service that creates revenue, royalties, rent or income from our content or its inclusion as part of a paid for service or for other commercial gain. Springer Nature journal content cannot be used for inter-library loans and librarians may not upload Springer Nature journal content on a large scale into their, or any other, institutional repository.

These terms of use are reviewed regularly and may be amended at any time. Springer Nature is not obligated to publish any information or content on this website and may remove it or features or functionality at our sole discretion, at any time with or without notice. Springer Nature may revoke this licence to you at any time and remove access to any copies of the Springer Nature journal content which have been saved.

To the fullest extent permitted by law, Springer Nature makes no warranties, representations or guarantees to Users, either express or implied with respect to the Springer nature journal content and all parties disclaim and waive any implied warranties or warranties imposed by law, including merchantability or fitness for any particular purpose.

Please note that these rights do not automatically extend to content, data or other material published by Springer Nature that may be licensed from third parties.

If you would like to use or distribute our Springer Nature journal content to a wider audience or on a regular basis or in any other manner not expressly permitted by these Terms, please contact Springer Nature at

onlineservice@springernature.com